

## Nanofiller in aircraft and heavy vehicles tyre rubber compounds

S. Ostad Movahed<sup>1\*</sup>, A. Ansarifar<sup>2</sup>

<sup>1</sup> Faculty of Sciences, Ferdowsi University of Mashhad, Mashhad, Iran

<sup>2</sup> Institute of Polymer Technology and Materials Engineering (Department of Materials) Loughborough University, Leicestershire, LE11 3TU, UK

### ABSTRACT

Natural rubber is the main polymeric base of aircraft and heavy vehicles tyre rubber compounds. The effect of the same amount of a silica nanofiller on the curing, mechanical and dynamic properties of natural rubber compounds was investigated. The silica surfaces were pre-treated with bis[3-triethoxysilylpropyl] tetrasulfide (TESPT) to chemically bond silica to rubber. The rubbers were primarily cured by using sulfur in TESPT, and the cure was optimized by the addition of accelerator and activator, which helped to form sulfur chemical bonds between the rubber and filler. Different amounts of accelerator and activator were needed to fully crosslink the filled rubbers. The mechanical and dynamical properties of the vulcanizates improved substantially by the incorporation of the filler in the rubber. This was due to high level of rubber-filler adhesion and formation of chemical bonds between the rubber and TESPT.

**Keywords:** Nanofiller , Rubber, Mechanical properties, Dynamical properties

### INTRODUCTION

The expansion and success of the rubber industry world-wide owes a great deal to the hard work and brilliance of rubber experts who over the years produced a wide range of rubber articles. On tapping the *Hevea brasiliensis* tree, natural rubber latex exudes, which has a rubber content between 25 to 40 per cent by weight.

The solid rubber or cis-1-4 polyisoprene (NR) is extracted from the latex. The useful properties of NR include high gum and tear strength, high abrasion resistance, long flex life and high resilience. Because of these excellent properties, NR is used in many industrial applications for example, tyres, belting, anti-vibration mountings, and bridge bearings. Synthetic polyisoprene (IR) is the synthetic analogue of NR, and is

chemically and structurally similar to it. IR has been used in the same applications as NR such as in blends with styrene-butadiene rubber and polybutadiene rubber to improve their processibility, and also mineral filled IR is used in footwear, sponge, and sporting goods [1].

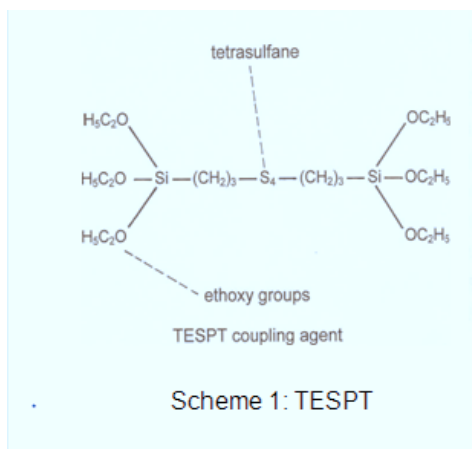
Raw rubbers often possess weak mechanical properties, and must be reinforced with fillers. Reinforcement increases properties for example

\* Correspondence to: S .Ostad Movahed ( s-ostad@um.ac.ir)

hardness, abrasion resistance, and tensile strength. Carbon blacks, synthetic silicas, quartz, and metal oxides, which have large surface areas ranging from 150 to 400 m<sup>2</sup>/g are very effective in improving the rubber properties [2]. The major disadvantage of silicas is their acidity [3] and polarity [4], which is caused by the presence of silanol groups on the silicas surfaces. This causes unacceptably long cure times and slow cure rates [5], and also loss of crosslink density in sulfur-cured rubbers [6]. Moreover, processing becomes more difficult when a large amount of silica is added because the viscosity increases significantly [7,8]. The availability of the coupling agent bis(3-triethoxysilylpropyl-)tetrasulfide (TESPT) has provided a better opportunity for using synthetic silicas to crosslink and reinforce rubbers. TESPT possesses tetrasulfane and ethoxy reactive groups (Scheme 1). The tetrasulfane groups react with the rubber in the presence of accelerators at elevated temperatures, i.e. 140-240°C, with or without elemental sulphur being present, to form crosslinks in unsaturated rubbers. The

ethoxy groups react with the silanol groups on the surfaces of silicas to form stable filler/TESPT bonds. Moreover, the number of silanol groups decreases after reaction with TESPT, and the remaining groups become less accessible to the rubber because of steric hindrance [5]. This weakens the strong interaction between silica particles [5], which reduces the viscosity of rubber compounds, and also improves cure properties by preventing acidic silicas from interfering with the curing reactions in sulfur-cured rubbers. It has been reported [9] that TESPT is a satisfactory property promoter in silica/NR composites through C-S bonding with rubber molecules. Precipitated silica pre-treated with TESPT is classified as a "crosslinking" filler. Parker and KOENIG [10] evaluated effects of silane pre-treated silica, and silica and liquid silane mixture on the crosslink density of a sulfur-cured rubber and concluded that the rubber with silane pre-treated silica had a higher crosslink density and increased filler-rubber adhesion. Ansarifard and co-workers [11,12] carried out a similar study and reached to the same conclusion. They also found that the mechanical properties of rubber improved more substantially with TESPT pre-treated silica nanofiller.

The aim of this study was to crosslink and reinforce the mechanical and dynamical properties of NR with the same loading of TESPT pre-treated silica nanofiller. The bound rubber content and crosslink density of the rubbers were also measured to assess the extent of rubber-filler adhesion and chemical bonding between the rubber and filler, respectively.



## EXPERIMENTAL

### Materials - Rubber, filler and rubber chemicals

The raw rubbers used were standard Malaysian natural rubber grade L (98 wt % cis-1-4 content; SMRL) and synthetic polyisoprene (minimum 96 wt % cis-1-4 content; Kraton IR-307, Kraton Polymers, USA). The reinforcing filler was Coupsil 8113 (Degussa Ltd., Hanau, Germany). Coupsil 8113 is precipitated amorphous white silica-type Ultrasil VN3 surfaces of which had been pre-treated with TESPT. It has 11.3% by weight TESPT, 2.5% by weight sulfur (included in TESPT), 175 m<sup>2</sup>/g surface area (measured by N<sub>2</sub> adsorption), and a 20-54 nm particle size.

### Curing chemicals, antidegradants and processing oil

In addition to the raw rubbers and filler, the other ingredients were *N*-t-butyl-2-benzothiazole sulfenamide (Santocure TBBS, Woluwe, Belgium; a safe-processing delayed action accelerator), zinc oxide (Harcros Durham Chemicals, UK; activator), stearic acid (Anchor Chemical Ltd, UK; activator), elemental sulfur (Solvay Barium Strontium, Hannover, Germany; curing agent), *N*-(1,3-

dimethylbutyl)-*N'*-phenyl-*p* phenylenediamine (Santoflex 13, Brussels, Germany; antidegradant). The cure system consisted of TBBS, zinc oxide, stearic acid, and elemental sulfur. TBBS, zinc oxide, and stearic acid were added to optimize the chemical bonding or crosslinks between the rubber and filler. Accelerators are ingredients used to control the onset and rate of cure and the crosslink density in rubber. Activators are chemicals used to enhance the effectiveness of the accelerators during the curing reaction in rubber. Elemental sulfur is a curing agent used to crosslink rubbers with unsaturation sites or chemically active double bonds such as natural rubber. In total, 58 compounds were prepared for this study.

### Mixing

The compounds were prepared in a Haake Rheocord 90 (Berlin, Germany), a small size laboratory mixer with counter rotating rotors. In these experiments, the Banbury rotors and the mixing chamber were maintained at 24°C and 48°C for making the IR and NR compounds, respectively, and the rotor speed was 45 r.p.m. The volume of the mixing chamber was 78 cm<sup>3</sup>, and it was half full. Haake Software Version 1.9.1. was used for controlling the mixing condition and storing data.

### Assessment of the silica dispersion in the rubbers

In order to select a suitable mixing time for incorporating the filler in the rubber, the rubber and filler were mixed together for different times. The filler was introduced first in the mixer, and then the raw rubber was added. The filler was added when the viscosity of

the rubber was still relatively high, which lead to an improved dispersion[13]. Following the previous findings [14] the mixing time was increased to 13 min to disperse the silica particles fully in the rubber. The temperature of the rubber compounds during mixing was 50-62°C. Twenty four hours after mixing ended, the rubbers were examined in an scanning electron microscope (SEM) to assess the filler dispersion. Dispersion of the silica particles in the rubber was assessed by a LEO 1530 VP Field emission gun scanning electron microscope (SEM). Small pieces of the uncured rubber were placed in liquid nitrogen for 3 min, and then fractured to create two fresh surfaces. The samples, 60 mm<sup>2</sup> in area and 5 mm thick, were coated with gold, and then examined and photographed in the SEM. The degree of dispersion of the silica particles in the rubber was subsequently studied from SEM photographs. After the SEM photos were examined, suitable mixing times were used for adding the filler to the rubbers.

#### Cure properties of the rubber compounds

The viscosity of the rubber compounds was measured at 100°C in a single-speed rotational Mooney viscometer (Wallace Instruments, Surrey, UK) according to the British Standard [15]. The results were expressed in Mooney Units (MU). The scorch time, which is the time for the onset of cure, and the optimum cure time, which is the time for the completion of cure, were determined from the cure traces generated at 140 ± 2 °C by an oscillating disc rheometer curemeter (ODR, Monsanto, Swindon, UK) at an angular displacement of ± 3 ° and a

test frequency of 1.7 Hz. [16] The cure rate index, which is a measure of the rate of cure in the rubber, was calculated using the method described in the British Standard [17]. The rheometer tests ran for up to three hours. The cure traces of the compounds which were subsequently used in this study are shown in Table 1.

Table 1: Formulations, Mooney viscosities and the ODR test results for the three compounds.

Compound No.	1*	2	3
NR(phr)	100	100	100
Coupsil (phr)	---	60	60
TBBS (phr)	6	6	6
ZnO (phr)	0.3	0.3	0.3
Sulphur (phr)	1.5	--	1.5
Santoflex 13	1	1	1
Min.Torque(dN.m)	12.2	25.8	26.8
Max.Torque (dN.m)	71.1	106.9	135.1
$\Delta torque$ (dN.m)	58.9	81.3	108.3
$t_{s1}$ (min)	21	8.1	5.5
$t_{90}$ (min)	32.5	23.5	9.1
$t_{95}$ (min)	34.3	26.6	9.2
CRI(min <sup>-1</sup> )	8.7	6.52	28.33
Mooney viscosity (MU)	49	97	106

\*Compound 1 is the control compound.

#### Test pieces and test procedure

After these measurements were completed, the rubber compounds were cured in a compression mould at 140 °C with a pressure of 11 MPa. Pieces of rubber, each approximately 140 g in weight, were cut from the milled sheet. Each piece was placed in the centre of the mould to enable it to flow in all the directions when pressure was applied. This prevented anisotropy from forming in the cured rubber. For

determining the mechanical properties of the rubber, sheets 23 cm by 23 cm by approximately 2.4 mm thick were used, from which various samples for further tests were cut.

#### Bound rubber and crosslink density measurement

The solvent used for the bound rubber and crosslink density determination was toluene. For the determination, 1.7 g (control compound) and 2 g (filled compound) of the rubber compounds were cured in a compression mould to produce cylindrical samples, 15.6 mm in diameter and 9.5 mm in height. The samples were then placed individually in 70 ml of the solvent in labelled bottles, and allowed to swell for 16 days at 21 °C. The weight of the samples was measured every day until it reached an equilibrium. It took approximately 8 days for the control compound and 5 days for the filled compounds to reach equilibrium. The solvent was removed after this time elapsed, and the samples were dried in air for 9 h. The samples were subsequently dried in an oven at 85 °C for 24 h, and allowed to stand for an extra 24 h at 23 °C before they were re-weighed. The bound rubber and crosslink density were then calculated using the expressions in References 18 and 19, respectively (Table 2).

#### Hardness

For measuring the hardness of the rubbers, cylindrical samples 12 mm thick and 28 mm in diameter, were used. The samples were then placed in a Shore A durometer hardness tester (The Shore Instrument & MFG, Co., New York) and the hardness of the rubber was measured at 23.5 °C over a 15-second interval after which a reading was taken. This was repeated at three different positions on the

sample, and median of the three readings calculated (Table 2)[20].

Table 2: Crosslink Density, Bound Rubber, and Mechanical Properties of the NR Rubber Vulcanizates

Compound No.	1	2	3
Hardness (Shore A)	52	77	75
Tensile strength (MPa)	18	34	37
Elongation at break (%)	1100	700	
837			
Stored energy density at break (MJ/m <sup>3</sup> )	59	109	
137			
T (kJ/m <sup>2</sup> )	15	57	
58			
Bound rubber (%)	-	94	
94			
Crosslink density (mol/m <sup>3</sup> )	96	178	
149			
$\Delta v$ (mm <sup>3</sup> /mg)	453	122	
73			
Modulus at different strain amplitudes (MPa)			
Strain amplitude (%)			
100	0.54	3.15	
2.23			
200	0.44	4.83	
3.16			
300	0.54	5.32	
4.23			

#### Cohesive tear strength

Rectangular strips, 100 mm long and 30 mm wide, were cut from the cured sheets of rubber and a sharp crack, approximately 30 mm in length, was introduced into the strips half way along the width and parallel to the length of the strip, to form the trouser test pieces for the tear experiments. The tear tests were performed at an angle of 180°, at ambient temperature (21°C) and at a constant cross-head speed of 50 mm/min [21] in a Lloyd mechanical testing machine (Hampshire, UK). The tears produced in the rubber after the test pieces were fractured were 14 to 79 mm in length.

In each experiment, the tearing force was recorded to produce traces from which an average force was measured. The first peak corresponds to the onset of crack-growth, where the tearing force was still rising, and the last peak corresponds to when test stopped or the sample broke. These were not considered. The remaining peaks on the trace were utilised for calculating an average tearing force for the rubber. In some cases, the test produced only one peak from which a tearing force was calculated. For each rubber, five test pieces were used. After these measurements were completed, and following the procedure described previously [22]. The force values were placed in Equation 1

$$T=2F/t \quad (1)$$

where F is the force, and t the thickness of the test piece, to calculate tearing energies, T, for the rubbers. The median values of the tearing energies were subsequently noted (Table 2).

#### **Tensile properties**

The tensile stress, elongation at break, and stored energy density at break of the rubbers were determined in uniaxial tension in a Lloyd mechanical testing machine, using dumbbell test pieces 75 mm long with a central neck 25 mm long and 3.6 mm wide. The test pieces were die-stamped from the sheets of cured rubber. The tests were performed at 21°C and at a cross-head speed of 50 mm/min [23]. Lloyd DAPMAT computer software was used for storing and processing the data (Table 2).

#### **Abrasion resistance**

For determining the abrasion resistance of the rubbers, moulded cylindrical test pieces, 8 mm thick and

16 mm in diameter, were cured. The tests were performed at 23 °C in accordance with BS 903: Part A9:1995 using method A.1 (Zwick abrasion tester 6102 and abrasion standard rubber S1) [24]. For each rubber, three samples were tested to calculate the relative volume loss ( $\Delta v$ ; Table 2).

#### **Loss tangent ( $\tan \delta$ ), Loss and storage modulus**

Tan  $\delta$  is the ratio between loss modulus and elastic modulus. The loss modulus represents the viscous component of modulus and includes all the energy dissipation processes during dynamic strain. The tan  $\delta$  was measured in DMAQ800 model CFL-50 (TA Instruments, USA), using Universal Analysis 2000 Software Version 4.3A. Test pieces 35 mm long, 13 mm wide and approximately 2.40 mm thick were used. The tests were performed at 1,10 and 100 Hz frequencies. The samples were deflected by 15, 256, 500 and 1000  $\mu\text{m}$  (nominal peak to peak displacement) during the test, and the sample temperature was raised from -80°C to 100°C at 3°C/min steps.

#### **Modulus at different strain amplitudes**

The modulus of the vulcanizates was measured at 100%, 200% and 300% strain amplitudes in uniaxial tension, using dumbbell test-pieces. The tests were carried out at ambient temperature ( $\sim 28^\circ\text{C}$ ) at a cross head speed of 50 mm/min in a Hounsfield mechanical testing machine (Hounsfield, Surrey, UK). QMAT-DONGLE version 2003 computer software was used to process the data (Table 2).

## **RESULTS AND DISCUSSION**

### Silica dispersion and effect of the filler on the rubber viscosity

To disperse the silica particles fully in the rubbers, the mixing time was increased to 13 min. Large silica aggregates were seen in the rubber matrix after short mixing times, e.g. 8 min (Fig. 1), and the filler dispersion improved as mixing time was increased to 13 min (Fig. 2), the silica particles were fully dispersed, and the size of the particles was down to about 60 nm. This was similar to the actual particle size of the filler, 20-54 nm, before it was mixed with the rubber. It was concluded that minimum mixing times of 13 min was sufficient to fully disperse the silica particles in the NR rubbers. The full dispersion of the silica particles in the rubber helped to maximize the reinforcing effect of the filler on the mechanical properties of the vulcanizates [25]. Long mixing time breaks down the rubber and causes reduction in molecular weight and viscosity [13,26]. The reduction is due to chain scission [27,28] or the mechanical rupture of the primary carbon-carbon bonds that are present along the backbone of the rubber chains. This is often compensated by the reinforcing effect of the filler. The viscosity of the NR rubber increased from 97 to 106 MU when the filler and curing chemicals were added (compound 2 and 3; Table 1). The control NR compound had a viscosity of 49 MU (compound 1; Table 1). Viscosity increases when additives such as fillers, elemental sulfur and activators are mixed with NR [13].

### Effect of nanofiller on the mechanical properties of the cured rubbers

The addition of the filler influenced the mechanical properties of the NR vulcanizates (cf. compounds 1 with 2 and 3; Table 2). The hardness and tensile strength increased from 52 to 75 Shore A and from 18 to 37 MPa, respectively. The modulus increased by a factor of 4 at 100% and approximately 8 at 200% and 300% strain amplitudes. This indicated a much stiffer rubber because of the filler. The abrasion resistance improved quite significantly with  $\Delta v$  decreasing from 453 to 73 mm<sup>3</sup>/mg. T and stored energy density at break were also up from 15 to 58 kJ/m<sup>2</sup> and from 59 to 137 MJ/m<sup>3</sup>, respectively, but elongation at break decreased from 1100 to 837% when the filler was added.

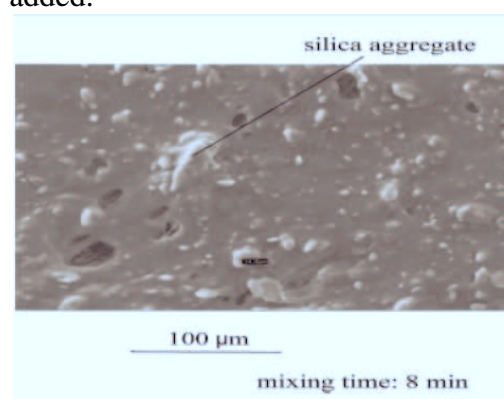


Figure 1. SEM photograph showing the dispersion of the silica in the rubber. Data for the NR rubber. Mixing time = 8 min with poor dispersion.

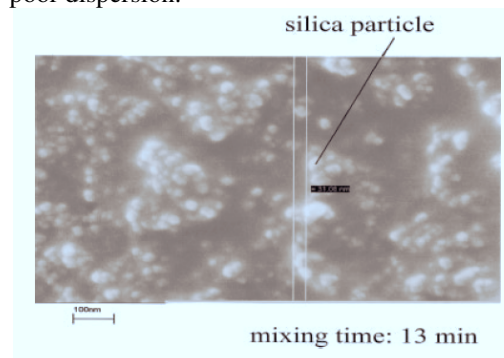


Figure 2. SEM photograph showing the dispersion of the silica particles in the rubber. Data for the NR rubber. Mixing time = 13 min with good dispersion.

### Effect of elemental sulfur on the mechanical properties of the filled NR rubber

The addition of elemental sulfur affected the rubber properties, although there was no overall advantage, as some properties improved and others deteriorated (cf. compound 2 with 3; Table 2). The hardness increased from 75 to 78 Shore A, and T remained almost unchanged at 57 kJ/m<sup>2</sup>. However the remaining properties were adversely affected. For example, the tensile strength decreased from 37 to 34 MPa, elongation at break from 837 to 700%, and stored energy density at break from 137 to 109 MJ/m<sup>3</sup>, respectively. Likewise,  $\Delta v$  increased from 73 to 122 mm<sup>3</sup>/mg, which indicated a significant deterioration in the resistance of the rubber to abrasion, and the modulus reduced by a factor of approximately 1.5 over a 300% increase in the strain amplitude.

### Dynamic properties of the nanosilica filled NR compounds

Although static mechanical properties have a great role in service life of tyre, enough attention should be paid to dynamic properties. In fact, wearing of the tyre along with its performance are two sides of the same coin. Figure 3 shows  $\tan \delta$  versus temperature at 1 Hz frequency for compound 2 in Table 1.

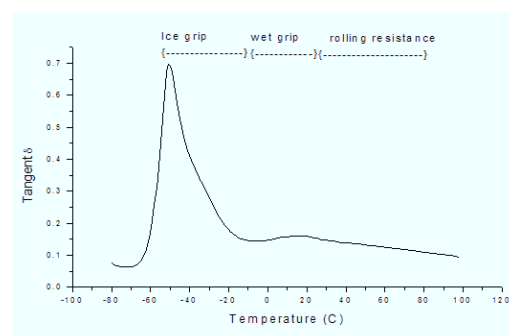


Figure 3:  $\tan \delta$  versus temperature for compound 2 in Table 1.

The regions where  $\tan \delta$  values correspond to ice-grip, wet-grip and rolling resistance of tyres are shown on the figure. From the viscoelastic property point of view [29], an ideal material, which is able to meet the requirement of a high-performance tyre should give low  $\tan \delta$  values at a temperature range of 50-80°C in order to reduce rolling resistance and save energy. The ideal material should also have high  $\tan \delta$  values or high hysteresis at lower temperatures for example less than -20°C in order to obtain high skid resistance and wet grip. However, the factors involved in skid resistance are recognized to be more complex than a single compound property. It is therefore evident that compound 2 satisfies all the requirements mentioned above. As can be seen in Figure 3, at sufficiently low temperatures, i.e. less than the Tg of the rubber, the  $\tan \delta$  value is very low (here about 0.05). This is due to the fact that the viscosity of the rubber is so high and the free volume in the polymer is so small that the movement of the polymer chain segments and the adjustment of their relative positions can hardly take place in the time scale involved in these experiments. Therefore, this results in a low energy

dissipation or absorption in the rubber and low loss modulus, hence low hysteresis or  $\tan \delta$ . Under this condition, the polymer falls in the glassy state with a very high storage modulus. With increasing temperature, the movement of the polymer chain segments increase. When the temperature reaches a certain level, i.e.  $T_g$ , the free volume of the polymer increases more rapidly than the volume expansion of the molecules, facilitating the segmental motion. Above  $T_g$ , the viscosity of the polymer decreases very rapidly and the molecular adjustment takes place more easily, so the storage or elastic modulus decreases. Simultaneously the energy dissipation within the polymer molecules increases with temperature, resulting in a high hysteresis or high  $\tan \delta$  values. At temperatures high enough, i.e. greater than  $50^\circ\text{C}$ , the Brownian motion is so rapid and viscosity is so low in the polymeric solid that the thermal energy is comparable to the potential energy barriers to segmental rotation, the molecular adjustment is quick enough to be able to follow the dynamic strain. Hence, long range contour changes of polymer molecules may take place and low resistance to strain. Now the material is in rubbery region with low energy dissipation or low loss modulus during dynamic deformation. Figure 4 represents  $\tan \delta$  versus temperature at 1, 10 and 100 Hz test frequencies and  $500 \mu\text{m}$  oscillation amplitude for the same compound.

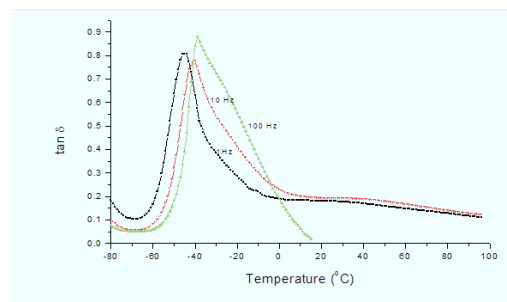


Figure 4:  $\tan \delta$  versus temperature for compound 2 in Table 1 at different frequencies and an oscillation amplitude of  $500 \mu\text{m}$ .

With increasing the test frequency from 1 to 100 Hz, the curves shifted to the right hand side towards higher temperatures. In addition, as the test frequency increased from 1 to 100 Hz, the  $\tan \delta$  values were noticeably higher at a given temperature above the peak  $\tan \delta$  values. This was the case for temperatures greater than  $-40^\circ\text{C}$  and up to  $0^\circ\text{C}$ . For example, at  $-20^\circ\text{C}$ , the  $\tan \delta$  values were 0.28, 0.42 and 0.58 at 1, 10 and 100 Hz, respectively. Evidently, an increase in the test frequency raised  $\tan \delta$  or energy dissipation in the rubber significantly, at least for temperatures up to  $0^\circ\text{C}$ . Thereafter,  $\tan \delta$  decreased sharply to approximately 0.02 at 100 Hz and very slowly to 0.12 at 1 and 10 Hz, respectively. Figure 5 shows  $\tan \delta$  versus temperature for compound 2 at three different frequencies and an oscillation amplitude of  $1000 \mu\text{m}$ . Before  $\tan \delta$  reached its peak, the  $\tan \delta$  values increased as a function of frequency. For instance, at  $-50^\circ\text{C}$ ,  $\tan \delta$  were 0.68, 0.34 and 0.21 at 1, 10 and 100 Hz, respectively. However, after  $\tan \delta$  reached its maximum value, the trend changed. For example,

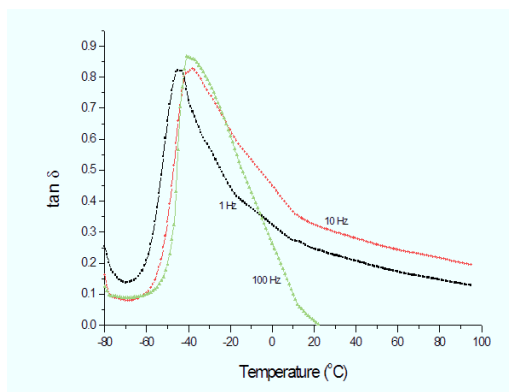


Figure 5:  $\tan \delta$  versus temperature for compound 2 in Table 1 at different frequencies at an oscillation amplitude of 1000  $\mu\text{m}$ .

at  $-30^\circ\text{C}$   $\tan \delta$  were 0.58, 0.76, and 0.79 as the test frequency was increased from 1 to 100 Hz, respectively. It was also noted that at about  $-8^\circ\text{C}$   $\tan \delta$  at 100 Hz continued decreasing sharply to 0. At 1 and 10 Hz,  $\tan \delta$  reduced at a slower rate to 0.14 and 0.19, respectively as the temperature reached  $100^\circ\text{C}$ . The peak  $\tan \delta$  values as a function of test frequency for 500 and 1000  $\mu\text{m}$  oscillation amplitudes are summarised in Table 3.

Table 3- Peak  $\tan \delta$  values as a function of test frequency. Data taken from Figures 4 and 5.

Test frequency	1 Hz	10 Hz	100 Hz
At 500 $\mu\text{m}$ oscillation amplitude			
Peak $\tan \delta$ value	0.85	0.76	0.87
At 1000 $\mu\text{m}$ oscillation amplitude			
Peak $\tan \delta$ value	0.82	0.82	0.86

At 500  $\mu\text{m}$  oscillation amplitude, this property was frequency dependent and decreased from 0.85 to 0.76 as the frequency was increased from 1 to 10 Hz, and then rose to 0.87 at 100 Hz. At 1000  $\mu\text{m}$  oscillation amplitude, this

property was unchanged with test frequency and was at 0.82, and then increased to 0.86 when the frequency was increased to 100 Hz. It seemed that increasing the test frequency and oscillation amplitude in some cases raises  $\tan \delta$  or energy dissipation in the rubber as a function of temperature. For example, at 500  $\mu\text{m}$ , the peak  $\tan \delta$  value increased from 0.85 to 0.87 when the test frequency was raised from 1 to 100 Hz. It was also noted that the results at 10 Hz did not follow the trend. Similarly, when the oscillation amplitude was increased from 500 to 1000  $\mu\text{m}$ , the peak  $\tan \delta$  value reduced from 0.85 to 0.82 at 1 Hz, and from 0.87 to 0.86 at 100 Hz. The result at 10 Hz followed an opposite trend, and it increased from 0.76 to 0.82. This is explained in terms of filler-filler and polymer-filler network break down and re-formation, which causes heat dissipation in the rubber. It means that as the test frequency and oscillation amplitude increase, the filler-polymer network breaks down and reforms more rapidly, and consequently more energy is dissipated in the rubber, giving rise to higher  $\tan \delta$  values. However, the exact reason for the unusual trend at 10 Hz is not immediately clear. Note also that at sufficiently low temperatures for example at  $-50^\circ\text{C}$ , the  $\tan \delta$  values at 1 Hz and oscillation amplitudes of 500 and 1000  $\mu\text{m}$  were 0.65 and 0.69, respectively. At 10 Hz, these values were almost the same at 0.34-0.35, and at 100 Hz, they were 0.17 and 0.22, respectively. At the same temperature above approximately  $-30^\circ\text{C}$ , the  $\tan \delta$  values were higher at higher frequencies and oscillation amplitudes. Clearly, the oscillation amplitude has a major effect on these measurements.

This will be investigated further. When the  $\tan \delta$  increments ( $\Delta \tan \delta$ ) were measured at the same oscillation amplitude and at different frequencies, for example at 500  $\mu\text{m}$  and at 1, 10 and 100 Hz, at high temperatures, e.g.  $-10^\circ\text{C}$ , they were 0.09 and 0.17, and at low temperatures, e.g.  $-50^\circ\text{C}$ , 0.13 and 0.46, respectively, which showed larger  $\Delta \tan \delta$  increases in the latter case. This is because at sufficiently low temperatures, in addition to heat dissipation produced by filler-filler and filler-polymer networks break down and reformation, polymer in situ, also has an important role in the processes causing heat dissipation. This can be further confirmed when we examine the  $\tan \delta$  results at 1 Hz and an increasing oscillation amplitudes. Figure 6 represents  $\tan \delta$  versus temperature at 1 Hz and 15, 256, 500 and 1000  $\mu\text{m}$  oscillation amplitudes for compound 2 in Table 1.

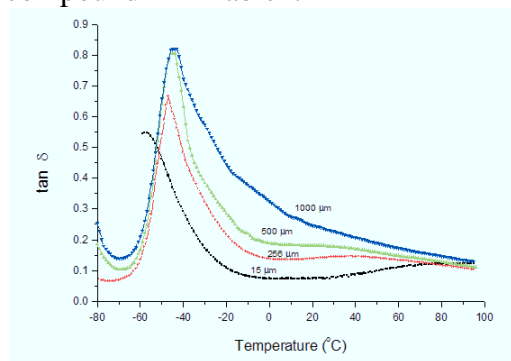


Figure 6:  $\tan \delta$  versus temperature at 1 Hz and 15, 256, 500 and 1000  $\mu\text{m}$  oscillation amplitudes. Data for compound 2 in Table 1.

It is clear that at higher temperatures, i.e. approximately above  $-50^\circ\text{C}$ ,  $\tan \delta$  increases as a function of the oscillation amplitude a lot more significantly than it does at lower temperatures, i.e. below  $-50^\circ\text{C}$ . This

confirms our previous findings namely that the oscillation amplitude as well as the test frequency affect the  $\tan \delta$  values. Figure 7 represents  $\tan \delta$  versus oscillation amplitude at 1 Hz and at  $-50$ ,  $-35$ ,  $-20$ ,  $0$ ,  $25$ ,  $45$ ,  $65$  and  $85^\circ\text{C}$  for compound 2 in Table 1. It is evident that the rate of increase of  $\tan \delta$  as a function of the oscillation amplitude depends on temperature. At

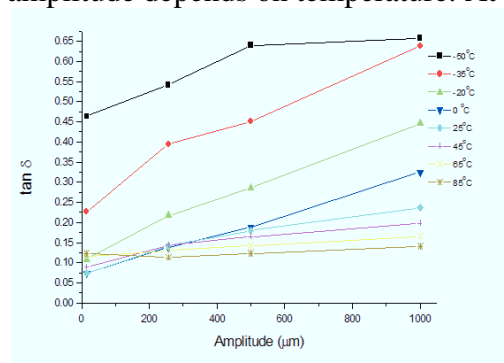


Figure 7 -  $\tan \delta$  versus oscillation amplitude at 1 Hz at different temperatures for compound 2 in Table 1.

low temperatures, i.e.  $0 - -50^\circ\text{C}$ ,  $\tan \delta$  increases at a faster rate. The lowest rate of increase occurs at  $65$  and  $85^\circ\text{C}$ . At high temperatures the polymer matrix is too rubbery to resist imposed strains. Indeed, polymer chains move in the same direction of the applied strain with the least resistance and consequently the heat dissipation in the rubber will be minimum. Hence, increasing the oscillation amplitude has little or no effect on the  $\tan \delta$  measurements. Figure 8 represents loss modulus,  $G''$  as a function of the oscillation amplitude at 1 Hz and  $-50$ ,  $-35$ ,  $-20$ ,  $0$ ,  $25$ ,  $45$ ,  $65$  and  $85^\circ\text{C}$  temperatures for compound 2 in Table 1.

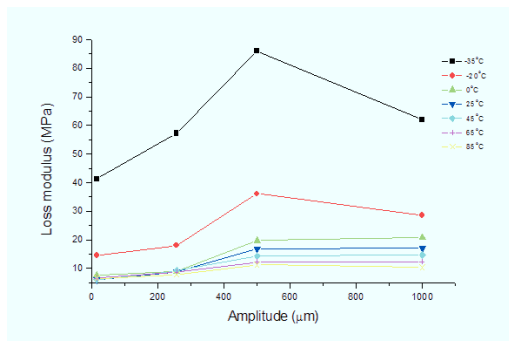
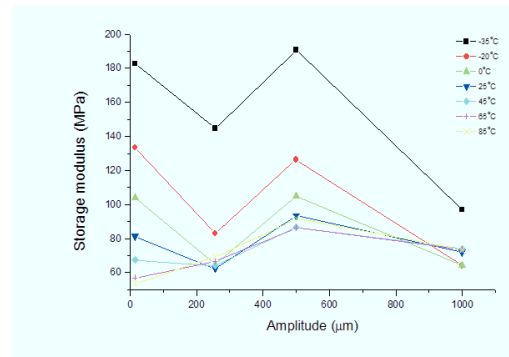


Figure 8 - Loss modulus versus oscillation amplitude for compound 2 in Table 1 at 1 Hz and different temperatures.

As it is evident, the loss modulus of the rubber reaches a maximum value at 500 μm oscillation amplitude irrespective of the temperature value. The loss modulus has the highest values at -35°C, reaching a peak and then dropping to lower values. This trend was also present at -20°C. As the temperature increases to 85°C, the loss modulus decreases progressively. Note also that the lowest values were recorded at 85°C. This behaviour confirms that at high temperatures heat dissipation is minimum because of the rubbery state of the material. Figure 9 shows storage modulus,  $G'$ , versus oscillation amplitude at 1 Hz and -50, -35, -20, 0, 25, 45, 65 and 85°C temperatures for compound 2 in Table 1.



amplitude of compound 2 in Table 1 at 1 Hz frequency and different temperatures.

It is interesting that the storage modulus decreases as the oscillation amplitude reaches 256 μm and then, it increases when the oscillation amplitude reaches 500 μm. Thereafter, it continues decreasing at different rates depending on the temperature value. For example, the largest decrease is recorded at -35°C and the smallest at 45-65°C. The only exception is at 65 and 85°C, where the storage modulus keeps increasing until the oscillation amplitude reaches 500 μm. Clearly, both temperature and oscillation amplitude have a large effect on the storage modulus. Figures 10 and 11 represent loss and storage modulus ( $G''$  and  $G'$ ) versus temperature at 1, 10 and 100 Hz and 500 μm oscillation amplitude for compound 2 in Table 1.

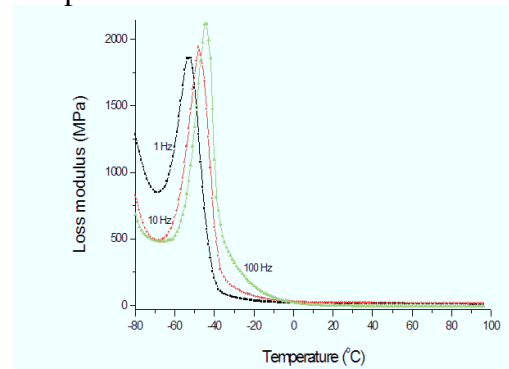


Figure 10 - Loss modulus versus temperature at different test frequencies. Data for compound 2 in Table 1 and oscillation amplitude of 500  $\mu\text{m}$ .

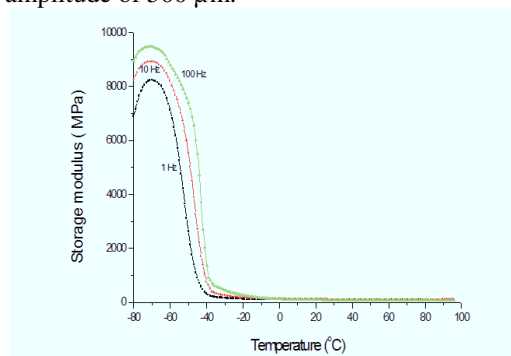


Figure 11 - Storage modulus versus temperature at different test frequencies and oscillation amplitude of 500  $\mu\text{m}$ . Data for compound 2 in Table 1.

Increases in test frequency shifts the storage and loss modulus to the right hand side or higher temperatures. The loss modulus decreases first as temperature increases to about  $-70^{\circ}\text{C}$  and then it rises sharply, reaching a peak at approximately  $-55$  to  $-40^{\circ}\text{C}$ . Thereafter, it drops to a much lower value at temperatures above  $-20^{\circ}\text{C}$  where temperature differences no longer affect it. Note that the peak values of the loss modulus were test frequency and temperature dependent and the lowest and highest values were at 1 and 100 Hz, respectively. In different way, storage modulus rises up to reach to a peak at  $-65^{\circ}\text{C}$  and then drops sharply for all studied frequencies. Figure 12 shows  $\tan \delta$  as a function of temperature for compounds 1, 2 and 3 at 1 Hz and an oscillation amplitude of 256  $\mu\text{m}$ . Compound 1 being the control compound (Table-1).

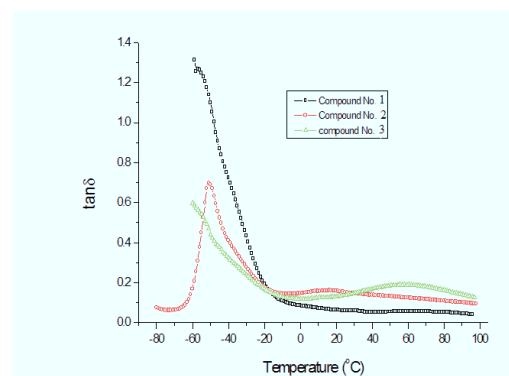


Figure 12:  $\tan \delta$  versus temperature for compounds 1 (control compound), 2 and 3 at 1 Hz and an oscillation amplitude of 256  $\mu\text{m}$ .

As it is clear from this figure, compound 1 has the largest peak  $\tan \delta$  value followed by compound 2. It is also noted that the compounds have the same  $\tan \delta$  values at about  $-20^{\circ}\text{C}$  and these values decrease slowly as the temperature was raised to  $100^{\circ}\text{C}$ . Over this temperature range, compound 1 has the lowest  $\tan \delta$  values. Compound 3 had extra crosslinks by the addition of elemental sulphur, whereas, compound 2 was cured primarily by the tetrasulphane groups of TESPT. Hence, the polymer chains were less mobile in compound 3 and this affected the  $\tan \delta$  of the compound at temperatures below and above  $-20^{\circ}\text{C}$ . At low temperatures up to  $T_g$ , the bulk of polymer (polymer in situ) is the dominant factor in its dynamic behaviour and responsible for most of the energy dissipation processes. When polymer is replaced with solid filler in compounds 2 and 3, at low temperatures, the low energy dissipation is due to the polymer chains trapped in the polymer-filler and filler-filler networks. In fact, trapped rubber at low temperature acts as a rigid glass substance and therefore is not rubbery, and the individual solid filler particles in the filler-filler

network in the polymer matrix do not absorb energy significantly. In contrast, at high temperatures the polymer-filler and filler-filler networks have significant effect on the energy dissipation processes in the rubber. There are two mechanisms involved in the filler-filler network behaviour as discussed by Wolff and Wang [30]. They named it 'direct contact mode' and 'joint shell mechanism' or 'junction rubber mechanism'. In most cases, both of these mechanisms are responsible for the filler-filler network dynamic behaviour. In direct contact mode, the break down and reformation of the filler network dissipate energy and consequently increase  $\tan \delta$ . For joint shell mechanism, at high temperatures the polymer matrix is in the rubbery state but the polymer in the rubber shell is in its transition zone caused by the adsorption of the polymer molecules on the filler surfaces or the interaction between the polymer chains and filler. In this case, the joint shell rubber would absorb more energy, resulting in higher hysteresis or  $\tan \delta$  due to an increase in energy dissipation in the rubber shell as well as in polymer matrix.

## CONCLUSIONS

From this study, it can be concluded that

- 1) The addition of elemental sulfur to the filled NR rubber with 6 phr TBBS and 0.3 phr zinc oxide increased the  $\Delta$ torque value, which indicated benefit for the crosslink density of the rubber. However, there was no overall advantage for the mechanical properties as some properties improved and others deteriorated.
- 2) The hardness, tensile strength, elongation at break, stored energy

density at break, T, abrasion resistance, and modulus of the rubber vulcanizates increased substantially when the filler was added. The improvement in the mechanical properties of the rubbers was mainly due to high level of rubber-filler adhesion and high crosslink density that was produced by the chemical bonding between the rubber and TESPT. The bound rubber measurements also confirmed a strong rubber-filler adhesion.

3) The dynamic properties of all the compounds were affected by the addition of silanized silica nanofiller. This fact was more evident when the glass transition temperatures of the gum (unfilled) NR with value  $-64^{\circ}\text{C}$  was compared with that of the filled rubber, which was  $-45^{\circ}\text{C}$ .

4) The superior mechanical and dynamical properties of filled rubbers make them a potential use in aircraft and heavy vehicles tyre rubber compounds.

## ACKNOWLEDGEMENT

The authors thank Loughborough Materials Characterisation Centre for performing the SEM of the samples. They also thank Degussa, Ltd., of Germany for supplying the filler and providing technical information on their product. The abrasion tests were carried out at COOPER TIRES, Ltd. (United Kingdom).

## REFERENCES

1. Hoffman, W. Rubber Technology Handbook; Carl Hanser Verlag, Munich, Germany, 1989.
2. Warrick, E. L.; Pierce, O. R.; Polmanteer, K. E.; Saam, J. C. *Rubber Chem Technol* 1979, 52, 437.
3. Hair, M. L.; Hertl, W. *J Phys Chem* 1970, 74, 91.

4. Hockley, J. A.; Pethica, B. A. *Trans Faraday Soc* 1961, 57, 2247.
5. Wolff, S.; Görl, U.; Wang, M. J.; Wolff, W., *Eur Rubber J* 1994, 16, 16.
6. Wolff, S. *Rubber Chem Technol* 1996, 69, 325.
7. Tan, E. H.; Wolff, S.; Haddeman, S. M.; Gretwatta, H. P.; Wang, M. J, *Rubber Chem Technol* 1993, 66, 594.
8. Dannenberg, E. M., *Rubber Chem Technol* 1975, 48, 410.
9. Thongsang, S.; Sombatsompop, N., *Polymer Composites*, 2006, 27, 30.
10. Parker, D. D.; KOENIC, J. L., *J Adhes* 2000, 73, 299.
11. Ansarifar, A.; Nijhawan, R.; Nanapoolsin, T.; Song, M., *Rubber Chem Technol* 2003, 76, 1290.
12. Ansarifar, A.; Azhar, A.; Song, M., *J Rubber Res* 2003, 6, 129.
13. Fries, H.; Pandit, R. R. *Rubber Chem Technol* 1982, 55, 309.
14. Cochet, P.; Barruel, P.; Barriquand, L.; Grobert, Y.; Bomal, Y.; PRat, E.; Rhone Poulenc, E., *Rubber World* 1994, 219, 20.
15. British Standards Institution, Methods of testing raw rubber and unvulcanized compounded rubber: Methods of physical testing. British Standard 1673: Part 3; London, UK, 1969.
16. British Standards Institution, Methods of test for raw rubber and unvulcanized compounded rubber: Measurement of pre-vulcanizing and curing characteristics by means of curemeter. British Standard 1673: Part 10; London, UK, 1977.
17. British Standards Institution, Methods of test for raw rubber and unvulcanized compounded rubber: Measurement of pre-vulcanizing and curing characteristics by means of curemeter. British Standard 903: Part A60: Section 60.1; London, UK, 1996.
18. Wolff, S.; Wang, M.; Tan, E. H., *Rubber Chem Technol* 1993, 66, 163.
19. Hamed, G. R.; Rattanasom, N., *Rubber Chem Technol* 2002, 75, 323.
20. British Standards Institution, Physical testing of rubber: Method for determination of hardness. British Standard 903: Part A26; London, UK, 1995.
21. British Standards Institution, Physical testing of rubber: Method for determination of tear strength trousers, angle and crescent test pieces. British Standard 903: Part A3; London, UK, 1995.
22. Greensmith, H. V.; Thomas, A. G., *J Polym Sci* 1955, 43, 189.
23. British Standards Institution, Physical testing of rubber: Method for determination of tensile stress strain properties. British Standard 903: Part A2; London, UK, 1995.
24. British Standards Institution, Method of testing vulcanized rubber. Determination of resistance to abrasion. British Standard 903: Part A9: Method A:1; London, UK, 1995.
25. Polmanteer, K. E. Lentz, C. W. *Rubber Chem Technol* 1975, 48, 795.
26. Harmon, D. J.; Jacobs, H. L., *J Appl Polym Sci* 1966, 10, 253.
27. Pike, M.; Watson, W. F., *J Polym Sci* 1952, 9, 229.
28. Ahagon, A. *Rubber Chem Technol* 1996, 69, 742.
29. Wang M J, *Rubber Chem. Technol.* 1998, 71, 521.
30. Wolff S, Wang M J., *Rubber Chem. Technol.* 1992, 65, 329.





